ACS APPLIED MATERIALS & INTERFACES

Research Article

www.acsami.org

Biotemplate Synthesis of Polyaniline@Cellulose Nanowhiskers/Natural Rubber Nanocomposites with 3D Hierarchical Multiscale Structure and Improved Electrical Conductivity

Xiaodong Wu, Canhui Lu, Haoyu Xu, Xinxing Zhang,* and Zehang Zhou

State Key Laboratory of Polymer Materials Engineering, Polymer Research Institute of Sichuan University, Chengdu 610065, China

Supporting Information

ABSTRACT: Development of novel and versatile strategies to construct conductive polymer composites with low percolation thresholds and high mechanical properties is of great importance. In this work, we report a facile and effective strategy to prepare polyaniline@cellulose nanowhiskers (PANI@CNs)/natural rubber (NR) nanocomposites with 3D hierarchical multiscale structure. Specifically, PANI was synthesized in situ on the surface of CNs biotemplate to form PANI@CNs nanohybrids with high aspect ratio and good dispersity. Then NR latex was introduced into PANI@CNs nanohybrids suspension to enable the self-assembly of PANI@CNs nanohybrids onto NR latex microspheres. During cocoagulation process, PANI@CNs nanohybrids selectively located in the interstitial space between NR microspheres and organized into a 3D hierarchical multiscale conductive network structure in NR matrix. The combination of the biotemplate synthesis of PANI and latex cocoagulation method significantly enhanced the electrical conductivity and mechanical properties of the NR-based nanocomposites simultaneously. The electrical conductivity of PANI@CNs/NR nanocomposites containing 5 phr PANI showed 11 orders of magnitude higher than that of the PANI/NR composites at the same loading fraction,; meanwhile, the percolation threshold was drastically decreased from 8.0 to 3.6 vol %.

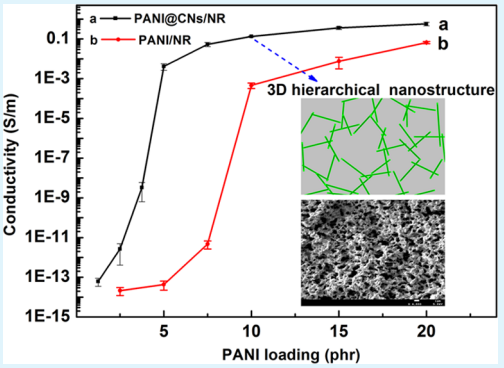

KEYWORDS: *cellulose nanowhiskers, natural rubber, composites, 3D hierarchical multiscale structure, electrical conductivity, mechanical properties*

INTRODUCTION

Conductive polymer composites (CPCs), especially conductive rubber composites, play an important role in the fields of antistatic material, electromagnetic shielding, pressure-sensitive sensors, overcurrent and overheating protection, etc. Typically, CPCs are prepared by adding conductive fillers, such as carbon black,[1] graphene,[2] carbon nanotube,[3] metal nanoparticles,[4] and intrinsically conductive polymers,[5−11] to polymer matrices. The widely used fabrication methods of CPCs are based on melt-blending,[1] solution mixing[4] and in situ polymerization.[12] However, high percolation threshold of conductive fillers is required to form continuous conductive network, which can lead to processing difficulty, deterioration of mechanical properties as well as high production cost of CPCs. Hence, how to prepare highly conductive CPCs with low amount of conductive fillers while retaining their good processability and mechanical properties has became one of the current critical issues.

For this purpose, several methods have been developed to lower the percolation thresholds of CPCs. For single polymer matrices, increasing the crystalline fraction of polymer matrices could facilitate the selective localization of conductive fillers in amorphous region, which promotes the formation of conductive pathways. Lower percolation thresholds can be achieved as a result.[13] For polymer blend matrices, controlling the dispersion of conductive fillers in interstitial space between immiscible polymers[14] or selectively locating conductive fillers in one phase[15] could enhance the conductivity of CPCs. However, the application of these methods is limited because of the noncrystalline characteristic of many other polymers (e.g., rubbers) and their mismatching of compatibility. Grunlan and co-workers[16,17] used clay as a template to assist the distribution of conductive fillers in epoxy, which led to the formation of conductive networks with lower conductive filler concentration. But the interaction between clay and conductive fillers was so weak that might be destroyed during polymer processing. Therefore, novel supporting or template materials that can establish strong interfacial interaction with conductive fillers are highly demanding for the production of high-performance CPCs.

Cellulose nanowhiskers (CNs), which derived from natural cellulose fibers by controlled acid hydrolysis, has attracted wide attention because of its unique properties: high aspect ratio, controlled morphology and surface chemistry, high specific

Received: September 2, 2014
Accepted: November 10, 2014
Published: November 10, 2014

strength and stiffness, and most importantly, the environmental sustainability. The high specific surface area, nanometric dispersity and good stability of CNs make it a promising biotemplate. Our previous work[18−20] demonstrated that as an excellent support for noble metal nanoparticles, CNs can effectively prevent their aggregation and thus significantly enhanced their catalytic properties. On the other hand, recent studies indicated that the −OH group in cellulose can form hydrogen bonding interaction with the −NH group of polyaniline (PANI),[21,22] which is an intrinsically conductive polymer with many potential applications because of its low-cost synthesis, simple doping/dedoping chemistry, high environmental stability, promising electronic and photoelectronic properties.[23−27] Therefore, CNs might serve as a good biotemplate to support and stabilize PANI for the fabrication of CNs-supported PANI (PANI@CNs) nanohybrids with high aspect ratio and good suspension property, which makes it easier to form continuous conductive network. In addition, CNs could "dilute" the conductive component because of the "volume-exclusion" effect,[28] allowing the formation of conductive structure with less conductive component.

Herein, we report a facile and effective strategy to fabricate PANI@CNs/natural rubber (NR) nanocomposites with 3D hierarchical multiscale conductive structure by the combination of the biotemplate synthesis of PANI and latex cocoagulation method.[29−33] In detail, a layer of PANI was in situ synthesized on CNs biotemplate to form PANI@CNs nanohybrids with high aspect ratio and good dispersity. Then PANI@CNs nanohybrids selectively located in the interfaces between NR microspheres and organized into a 3D hierarchical multiscale conductive network structure by cocoagulation. Hence, a novel hierarchical multiscale PANI@CNs/NR nanocomposite with low percolation thresholds and high mechanical strength was successfully prepared. To the best of our knowledge, this is the first report of constructing 3D hierarchical conductive rubber nanocomposites through the combination of CNs-assisted biotemplate synthesis and latex cocoagulation method.

MATERIALS AND METHODS

Materials. Analytical grade aniline (≥99.5%), ammonium persulfate (APS, ≥98%), sulfuric acid (H_2SO_4, 95−98 wt %), ammonium hydroxide ($NH_3{\cdot}H_2O$, 25−28%), toluene (≥99.5%), stearic acid (≥99.0%), OP emulsifier-10 (≥99.0%), and zinc oxide (≥98.0%) were all purchased from Chendu Kelong Chemical Reagent Company (China) and used without further purification. The NR latex (solid content: 58 wt %) was provided by Chengdu Xinyuanding Co., Ltd. (China). Medical purified cotton was obtained from Xuzhou Health Factory Co., Ltd. (China). Bovine serum albumin (BSA) was purchased from Shanghai Ruji Biology Technology Co., Ltd. (China). Vulcanization agent sulfur (≥98%) and accelerator N-cyclohexyl-2-benzothiazolesulfenamide (CBS, active content: ≥80%) were purchased from Weihai Tianyu New Mstar Technology Co., Ltd. (China).

Preparation of CNs. Cellulose nanowhiskers (CNs) were prepared by controlled acid hydrolysis of cotton fibers based on our previous studies.[19,20] Medical purified cotton (40 g) was mixed with sulfuric acid solution (700 mL, 64 wt %) and the mixture was stirred vigorously at 45 °C for 45 min. The suspension was diluted 6.4 times to stop the hydrolysis immediately after hydrolysis. Then the suspension was dialyzed to remove residual acid and hydrolysate of cellulose in the suspension. The result was monitored by checking the neutrality of the dialyzate. The dialysis membrane is made from regenerated cellulose with a molecular weight cut off of 100 000. Finally, the suspension was sonicated for 30 min at room temperature to disperse the aggregation. The solid content of the CNs suspension was measured 5 times and the mean value was 0.47 ± 0.02 wt %.

Preparation of PANI@CNs Nanohybrids and Neat PANI. In this study, PANI@CNs nanohybrids was synthesized through in situ oxidative polymerization of aniline using APS as oxidant and CNs as biotemplate in aqueous medium. In a typical experiment, 7.52 g aniline was added into a mixture of 400 mL of CN suspension (containing 1.88 g CNs) and 0.2 mol of H_2SO_4. Then the mixture was vigorously stirred to dissolve the aniline monomer and was sonicated for 60 min to allow the monomer to self-assemble onto the surface of CNs via hydrogen bonding, after which the reaction system was stirred in ice−water bath. After the temperature was cooled to 0 °C, 9.12 g APS was added into the reaction system with magnetic stirring. The suspension color changed from milk white to green after the polymerization was initiated. The polymerization proceeded in ice−water for 3 h and the final color of suspension changed to dark green. The obtained product was filtered and washed 3 times with distilled water to remove the byproducts and remaining reagents, followed by washing with 1 M $NH_3{\cdot}H_2O$ and distilled water to dedope the doping H_2SO_4 in PANI@CNs nanohybrids, which can cause coagulation of NR latex. The final PANI@CNs nanohybrids was diluted to 400 mL again. The solid content of the PANI@CNs nanohybrids suspension was measured 5 times and the mean value was 1.17 ± 0.02 wt %. Neat PANI was synthesized in the absence of CNs and all other conditions were in accordance with PANI@CNs nanohybrids. The solid content of the neat PANI suspension was measured 0.68 ± 0.05 wt %.

Preparation of PANI@CNs/NR and PANI/NR Nanocomposites. For the preparation of PANI@CNs/NR nanocomposites, the desired amount of PANI@CNs nanohybrids suspension was diluted to 250 mL (the pH value was adjusted to 9 with 1 M $NH_3{\cdot}H_2O$) and sonicated for 6 min to disperse the aggregation. Simultaneously, 8.6 g of NR latex was diluted to 250 mL and stirred for a while. Then the 250 mL of sonicated PANI@CNs nanohybrids suspension and 250 mL of NR latex, as well as an aqueous suspension containing cross-linking agent sulfur and other additives, were mixed uniformly, forming a purple mixture. The experimental vulcanization formula is given in Table 1. The final purple mixture was coagulated by adding 150 mL of H_2SO_4 (1 M), meanwhile the dedoped PANI on CNs was doped again by H_2SO_4 (The conductivity of redoping PANI@CNs was measured to be 4.1 S/m). After filtering, the solid mixture was soaked in renewed distilled water to remove the residual H_2SO_4 and finally dried at 60 °C for 12 h. The dried composites were cut into pieces, molded using compression molding (45 mm × 10 mm × 1 mm) and vulcanized at a temperature of 150 °C and a pressure of 10 MPa for 5 min. The PANI/NR composites were prepared following the same procedure of the above PANI@CNs/NR nanocomposites. Hereinafter, in the PANI@CNs/NR (or PANI/NR) composites, phr means parts per hundred parts of natural rubber.

Table 1. Experimental Vulcanization Formula for Preparation of PANI@CNs/NR and PANI/NR Nanocomposites

	NR	zinc oxide	stearic acid	sulfur	CBS	OP emulsifier
content (phr[a])	100	3	1.8	1.68	0.9	0.25

[a]Parts per hundred parts of natural rubber.

Extraction of PANI@CN Nanohybrids Skeleton from PANI@CNs/NR Nanocomposites. To intuitively observe and evaluate the 3D hierarchical multiscale conductive network fabricated with PANI@CNs nanohybrids in NR matrix by cocoagulation and hot pressing, we etched unvulcanized NR composites with toluene to remove the NR matrix. The PANI@CNs/NR sample (20/15/100 wt./wt./wt., prepared without vulcanization) was extracted (Soxhlet extraction) by toluene for 48 h. The extracted PANI@CNs nanohybrids skeleton was dried in a drying oven at 60 °C for 12 h.

CHARACTERIZATION

Transmission electron microscopy (TEM) was performed using a transmission electron microscope (JEOL JEM-100CX, Japan). Diluted CNs and PANI@CNs nanohybrids aqueous suspensions were sonicated for 30 min to disperse the aggregation. The well dispersed CNs and PANI@CNs nanohybrids suspensions were directly dropped on a copper grid for observation. The diameter of pristine CNs and PANI@CNs nanohybrids were measured using Image-J software and at least 100 particles from different TEM images were analyzed.

Zeta potential of the pristine CNs (CNs were dispersed in deionized water with concentration of 0.235 mg/mL and pH value of 6.8) was measured using Zetasizer nano-ZS (Malvern, UK).

For Fourier transform infrared spectroscopy (FT-IR) studies, CNs and PANI@CNs nanohybrids suspensions were freeze-dried and then dried at 60 °C in air-circulating oven for 12 h. FT-IR analysis was conducted using a Nicolet 6700 spectrophotometer (USA). The powdered samples of CNs and PANI@CNs nanohybrids were mixed with KBr to produce tablets for FT-IR measurement. The spectra were recorded from 4000 to 400 cm^{-1} at a resolution of 2 cm^{-1}.

For suspension property evaluation, 0.5 g PANI or PANI@CNs nanohybrids suspension was diluted to 50 mL (the pH value was adjusted to 9 with 1 M $NH_3{\cdot}H_2O$) and sonicated for 30 min to disperse the aggregation. A desired amount of the sonicated PANI or PANI@CNs nanohybrids suspension was put into a vial and stood for 12 h. Digital pictures of PANI or PANI@CN nanohybrid suspensions were taken before and after the standing.

Preparation of drop-cast samples of CNs/NR for TEM measurements: 21.4 g of CNs suspensions (0.47 wt %) and 1.72 g of NR latex (58 wt %) were mixed and diluted. The mixture of CNs and NR latex was stirred and sonicated adequately for uniform mixing. The mixture was put on the copper grids and the water was evaporated. Then CNs in the drop-cast CNs/NR film was negatively stained with 1.5 wt % aqueous uranyl acetate solution for imaging purposes. The final sample was observed using a transmission electron microscope (JEOL JEM-100CX, Japan).

Scanning electron microscopy (SEM) was performed with a microscope (JSM-5900LV, JEOL, Japan). The NR-based nanocomposites as well as the dried extracted PANI@CNs nanohybrids skeleton were soaked in liquid nitrogen and fractured. The surface was sputter-coated with a thin layer of Au for SEM imaging.

The electric conductivity of all samples were measured on undeformed samples by a two-point measurement with a resistance meter (UT61, Uni-Trend, China) for $R \leq 2 \times 10^8$ Ω or using ZC36 high resistance instrument for $R > 2 \times 10^8$ Ω. A rectangle strip samples (40 mm × 10 mm × 1 mm) or square samples (100 mm × 100 mm × 1 mm) were used for electrical measurement. Five specimens were measured for each sample to achieve an average value. The measured volume resistance (Ω), R_v was converted to volume resistivity, ρ_v according to ASTM D4496 and D257 using the formula

$$\rho_v = R_v \frac{A}{t}$$

Where A is effective area of the measuring electrode (m^2) and t is specimen thickness (m).

Mechanical properties measurement was conducted on a versatile testing machine (ASTM D412−80) at room temperature. The rectangle specimens (40 mm × 10 mm × 1 mm) were stretched at a crosshead rate of 100 mm/min. The stress−strain curves were recorded. Five specimens were measured for each sample to achieve an average value.

RESULTS AND DISCUSSION

Biotemplate Synthesis of PANI@CNs Nanohybrids. CNs was derived from bulk cellulose by controlled acid hydrolysis of cotton fibers. A small amount of sulfate ester groups were introduced onto the surface of CNs during the sulfuric acid hydrolysis, which could electrostatically stabilize CNs. The zeta potential of CNs was measured to be −37.3 mV, which demonstrates excellent suspension property of CNs. Oxidative polymerization of aniline monomer was initiated with the addition of APS in ice−water bath. Without CNs, aniline monomer was polymerized into PANI particles, which resulted large-scale aggregation with several micrometers (see Figure S2b in the Supporting Information) to decrease their surface energy. When CNs were introduced, the large amount of hydroxyl groups on the CNs might interact with amine groups of aniline monomer via hydrogen bonding,[34,35] which led to the self-assembly of aniline monomer onto CNs. With the addition of APS, biotemplated polymerization of aniline monomer was initiated on CNs and the $\pi-\pi$ stacking of benzene ring led to the PANI chains grow parallel on CNs, giving cofacial layered PANI thin film deposited on the surface of CNs template[36] and forming the well-dispersed CNs-supported PANI nanohybrids.

TEM observation was employed to investigate the microstructure of pristine CNs and PANI@CNs nanohybrids. As shown in Figure 1a, needlelike CNs with the length of about

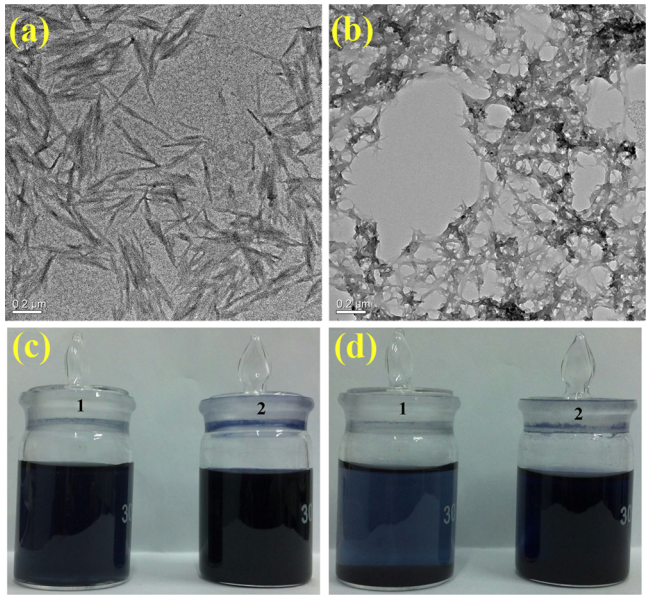

Figure 1. TEM images of (a) pristine CNs (scale bar, 0.2 μm) and (b) PANI@CNs nanohybrids (scale bar, 0.2 μm); digital pictures of (1) PANI and (2) PANI@CNs nanohybrid suspensions in water (c) before and (d) after standing for 12 h.

200−500 nm could be clearly observed. After in situ polymerization of aniline monomer onto CNs, the PANI@CNs nanohybrids was well dispersed and presented rod-like morphology (Figure 1b). Large-scale aggregation of PANI was not observed. The mean diameter of pristine CNs is about 16 ± 4 nm, whereas the mean diameter of PANI@CNs nanohybrids increased to 27 ± 8 nm, indicating that CNs template was coated with a layer of PANI. Atomic force microscopy image (as shown in Figure S1 in the Supporting Information) also confirmed the rodlike morphology of PANI@CNs nanohybrids. The results indicate that PANI was uniformly coated on the surface of CNs as a thin layer because of the template effect of CNs during polymerization. Wang et al.[34] showed that PANI could be deposited onto bacterial cellulose (BC) nanofibers but in the form of PANI particles. In addition, flakelike PANI particles have been synthesized via in situ polymerization of aniline monomer onto BC nanofibers scaffold.[35] In this work, however, a uniform layer of PANI

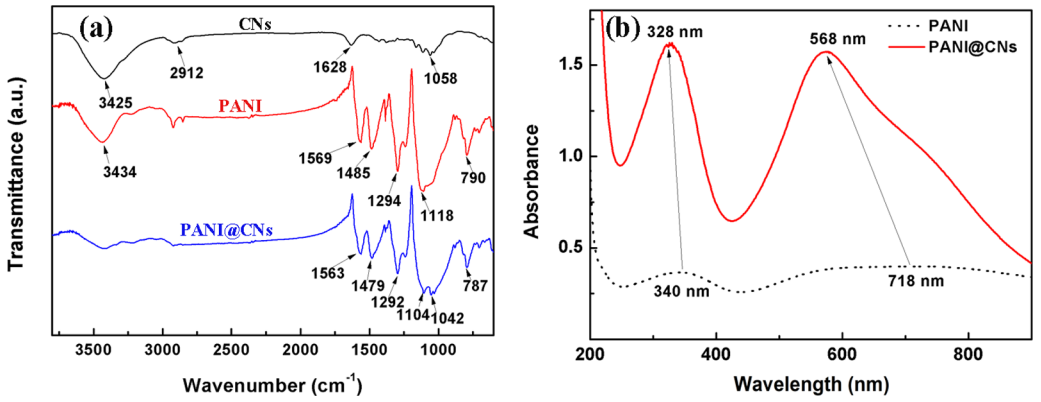

Figure 2. (a) FT-IR spectra of pristine CNs, neat PANI and PANI@CNs nanohybrids; (b) UV−vis spectra of neat PANI and PANI@CNs nanohybrids in aqueous suspension (PANI concentration: 0.04 mg/mL).

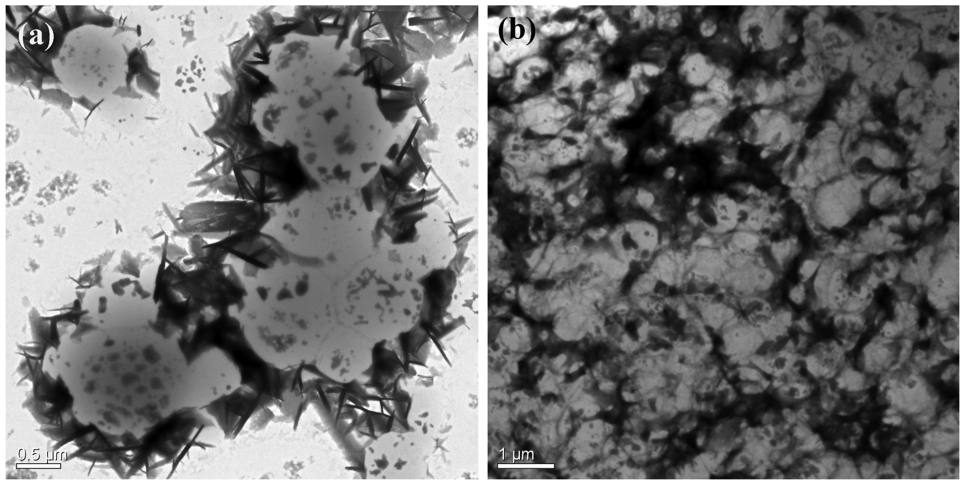

Figure 3. TEM images of CNs/NR nanocomposites prepared by self-assembly of CNs and NR latex microspheres, scale bars: (a) 0.5 μm and (b) 1 μm.

was coated on CNs and continuous nanosheath of PANI was developed on the biotemplate, which is of great advantage for higher conductivity of the PANI@CNs nanohybrids. This might be attributed to the difference in polymerization conditions (such as mass ratio of aniline monomer/nanocellulose, molar ratio of APS/aniline monomer, concentration of APS and aniline, polymerization temperature and so on). Low polymerization rate facilitates the gradually uniform growth of PANI on nanocellulose, whereas high polymerization rate results in PANI nanoparticles adsorbed on nanocellulose. The mass ratio of aniline monomer/nanocellulose and molar ratio of APS/aniline monomer were 4/1 and 0.5/1 in this work, which were much lower than that used in ref 34 (373/1 and 2.5/1). Thus, PANI was slowly polymerized and grew uniformly on CNs, resulting a uniform layer of PANI (not PANI particles) coated on CNs.

For suspension property evaluation, the suspensions of neat PANI and PANI@CNs nanohybrids were sonicated to disperse the aggregation. After sonication, PANI@CNs nanohybrids were rodlike and homogeneously dispersed. No visible particles were recognized in PANI@CNs suspension, while small particles of PANI were visible to naked eyes in PANI suspension. After standing for 12 h, the PANI suspension showed significant sedimentation of particles, whereas the PANI@CNs nanohybrids suspension remained stable as shown in Figure 1d. The difference in suspensions property of neat PANI and PANI@CNs nanohybrids could be attributed to their different particle size (see Figure S2b, c in the Supporting Information). This result suggests that CNs served as a good biotemplate for the dispersion and stabilization for PANI@CNs nanohybrids.

FT-IR analysis was carried out to study the chemical structure of pristine CNs, neat PANI and PANI@CNs nanohybrids. As can be seen in Figure 2a, pristine CNs presents characteristic bands around 3425 and 2912 cm^{-1}, which are attributed to the O−H stretching and C−H stretching in cellulose, respectively. The band at 1628 cm^{-1} is ascribed to the H−O−H bending of the absorbed water. The strong bands at 1058−1160 cm^{-1} is due to the C−O−C pyranose ring skeletal vibration.[37] The characteristic bands of neat PANI can also be observed clearly. The bands at 3434 and 1118 cm^{-1} arise from N−H stretching vibration. Peaks at 1569 and 1485 cm^{-1} could be attributed to the stretching of quinoid and benzenoid ring, respectively.[34] The FT-IR spectrum of PANI@CNs nanohybrids seems like a superposition of the FT-IR curves of neat CNs and PANI. However, the intensity of the O−H stretching band of CNs at 3425 cm^{-1} and N−H stretching band of PANI at 3434 cm^{-1} decreased dramatically. On the other hand, peaks for CNs (1042 cm^{-1}) and PANI (1563, 1479, 1104 cm^{-1}) in PANI@CNs nanohybrids shifted to lower wavenumbers compared to the neat CNs (1058 cm^{-1}) and PANI (1569, 1485, 1118 cm^{-1}). These results all suggest

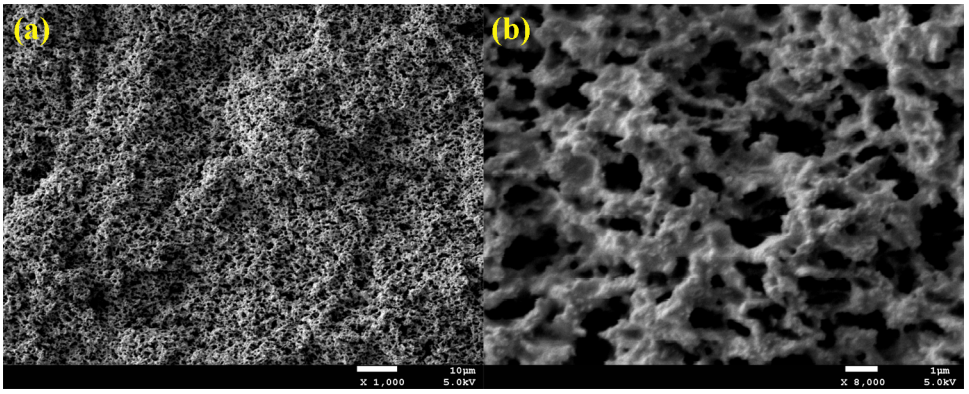

Figure 4. SEM images of the extracted PANI@CNs nanohybrids skeleton from PANI@CNs/NR nanocomposites by toluene, scale bars (a) 10 μm and (b) 1 μm.

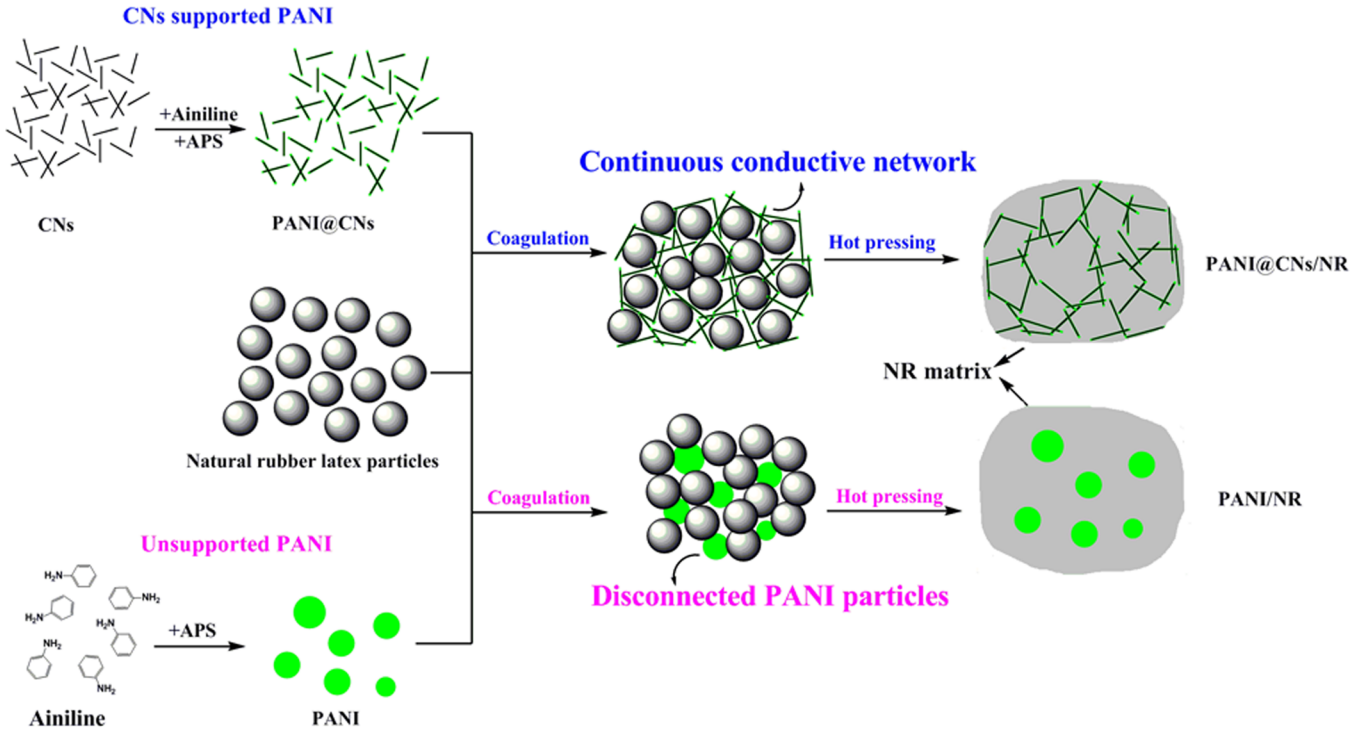

Figure 5. Schematic illustration for the preparation of PANI@CNs/NR nanocomposites with a 3D hierarchical multiscale structure.

that CNs formed strong interfacial interaction with the decorated PANI layer. It might be ascribed to the hydrogen bonding interaction between −OH of CNs and −NH of PANI.[22]

Furthermore, we used UV−vis spectrum to characterize the neat PANI and PANI@CNs nanohybrids (Figure 2b). At the same PANI concentration (0.04 mg/mL), the absorption peak of PANI suspension is much weaker than that of PANI@CNs nanohybrids, because PANI was poorly dispersed in water and usually precipitated out as large aggregation. For comparison, the much higher absorbance of CNs-supported PANI suspension indicates enhanced dispersity of PANI by CNs. The dedoped PANI showed two absorption peaks at 340 and 718 nm. The first peak at 340 nm is due to the $\pi-\pi^*$ transition of the benzenoid rings and the second broad peak at 718 nm is assigned to the n-π^* transition of the quinonoid rings of PANI.[38] However, the $\pi-\pi^*$ transition and the n−π^* transition bands of PANI supported on CNs blue-shifted to 328 and 568 nm, respectively. This might be attributed to the interaction arising from the hydrogen bonding between CNs and PANI,[39] which demonstrates that CNs is an effective and robust biotemplate for supporting conductive PANI.

Morphology Observation. To investigate the template effect of CNs, we observed the morphology and network formed by mixing CNs and NR latex using TEM. As shown in Figure 3a, CNs self-assembled and coated on the surface of NR latex microspheres, which have a diameter of several hundred nanometers. In addition, several NR latex microspheres encapsulated in CNs layers can also be observed clearly, which was beneficial to the formation of continuous network with less CNs. The CNs shells coated on NR latex microspheres were the prototype of the CNs network. During drying or cocoagulation procedure, these CNs coated NR latex microspheres connected with each other. As a result, CNs was selectively located in the interstitial space between the NR latex microspheres and organized into a continuous network as seen in Figure 3b. This interconnected network, built up from

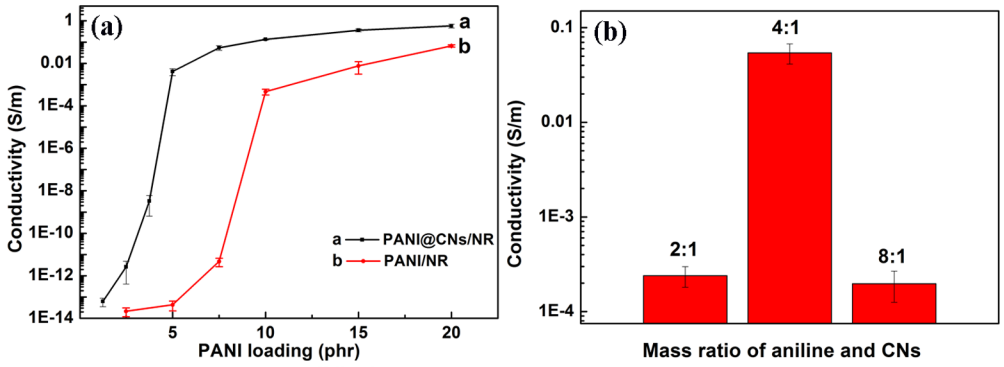

Figure 6. (a) Electrical conductivity of PANI/NR and PANI@CNs/NR nanocomposites as a function of PANI content; (b) effect of feeding mass ratio of aniline and CNs on the electrical conductivity of PANI@CNs/NR nanocomposites containing 7.5 phr PANI.

individual CNs, might serve as a prototype of a 3D hierarchical conductive network in NR matrix.

To intuitively observe and evaluate the 3D hierarchical multiscale conductive network fabricated with PANI@CNs nanohybrids in NR matrix by cocoagulation and hot pressing, we etched unvulcanized NR composites with toluene to remove the NR matrix. The residual PANI@CNs nanohybrids skeleton is shown in Figure 4. A uniformly porous network of PANI@CNs nanohybrids is observed in Figure 4a, suggesting that the 3D hierarchical structure was maintained during the hot pressing process. The pore diameter varies from several hundred nanometers to several micrometers (Figure 4b), which resulted from the extraction of one or several NR latex microspheres. This uniform porous network arises from the good dispersity of PANI@CNs nanohybrids and their selective location in the interstitial space between NR microspheres. Moreover, the extracted PANI@CNs nanohybrids skeleton was flexible and the residual weight of the network was higher than that of the PANI@CNs nanohybrids filler, indicating that the removal of NR was incomplete and some NR residue remained on the PANI@CNs nanohybrids skeleton because of the strong interfacial interaction between PANI@CNs nanohybrids and NR matrix. This 3D hierarchical conductive network is expected to realize the enhancement of electrical conductivity and mechanical properties of the PANI@CNs/NR nanocomposites.

Formation Mechanism of the 3D Hierarchical Multiscale Structure. According to the aforementioned discussion, the probable mechanism of this new approach to the biotemplate synthesis of PANI@CNs/NR nanocomposites with a 3D hierarchical multiscale conductive structure is schematically illustrated in Figure 5. In the presence of CNs, PANI was uniformly grown on the surface of CNs biotemplate during the in situ polymerization. Thus, CNs directed the growth of PANI into rod-like PANI@CNs nanohybrids with high aspect ratio and hindered the aggregation of PANI. Then NR latex was introduced into PANI@CNs nanohybrids suspension to enable the self-assembly of PANI@CNs nanohybrids onto NR latex microspheres as shown in Figure S2e (the self-assembly procedure is discussed in the Supporting Information). During the subsequent cocoagulation process, PANI@CNs nanohybrids was selectively located in the interstitial space between the NR latex microspheres and formed a 3D hierarchical multiscale conductive structure. On the contrary, in the absence of CNs, PANI particles were observed surrounded by NR latex microspheres (see Figure S2d in the Supporting Information) because of their large size and poor dispersity, which made it difficult for the PANI particles to connect with each other. Thus, PANI particles in NR matrix were disconnected and failed to form continuous conductive networks. Hence, the incorporation of CNs into PANI/NR composites played a key role in assisting the fabrication of the 3D hierarchical multiscale conductive structure.

Electrical Conductivity. The conductivity of PANI/NR and PANI@CNs/NR nanocomposites with different loading of PANI is shown in Figure 6a. The PANI@CNs nanohybrids were synthesized using a fixed feeding mass ratio of aniline/CNs (4/1) and the final mass ratio of PANI/CNs was 1.5/1. The critical content of conductive fillers required to cause the insulator-to-conductor transition is known as the percolation threshold. PANI@CNs/NR nanocomposites showed much lower electrical conductivity percolation threshold (3.8 phr, 3.6 vol %) than that of PANI/NR composites (8.8 phr, 8.0 vol %). In addition, significant conductivity enhancement is observed for all samples. For example, the electrical conductivity of the PANI/NR composite containing 5 phr PANI is 3.5×10^{-14} S/m, while for PANI@CNs/NR nanocomposite at the same loading fraction it reaches 3.8×10^{-3} S/m, showing an significant enhancement of 11 orders of magnitude. The enhanced conductivity can be attributed to the biotemplate effect of CNs and the 3D hierarchical multiscale conductive structure in NR matrix.

The influence of mass ratio of PANI to CNs on the electrical conductivity of PANI@CNs/NR nanocomposites was investigated by adjusting the feeding mass ratio of aniline to CNs in polymerization. The feeding mass ratio of aniline/CNs was 2/1, 4/1, and 8/1, respectively. The final mass ratio of PANI/CNs was 0.8/1, 1.5/1, and 2.6/1, indicating that the amount of PANI deposited on CNs increased with increasing mass ratio of aniline/CNs. The effect of feeding mass ratio of aniline to CNs on the electrical conductivity of PANI@CNs/NR nanocomposites containing 7.5 phr PANI can be seen in Figure 6b. The electrical conductivity reached the maximum 5.4×10^{-2} S/m when the feeding mass ratio of aniline/CNs was 4/1. However, with the feeding mass ratio of aniline/CNs decreased to 2/1 and increased to 8/1, the conductivity dropped to 2.4×10^{-4} and 2.0×10^{-4} S/m, respectively. It is believed that the electrical conductivity of PANI@CNs/NR nanocomposites is influenced by the amount of PANI deposited on CNs. With a small amount of PANI deposited on CNs, the PANI nanosheaths on CNs were disconnected. As a result, the conductive pathways formed in NR matrix were discontinuous. On the contrary, with too much PANI deposited on CNs, the PANI nanosheaths were continuous but too thick, which

weakened the template effect of CNs to some extent. Only with an appropriate amount of PANI on CNs can the interconnected network of PANI and the template effect of CNs be realized simultaneously.

Mechanical Properties. Tensile testing was employed to investigate the influence of PANI and PANI@CNs nanohybrids on the mechanical properties of the NR-based nanocomposites. Figure 7 shows the representative stress−strain curves of the pure NR, PANI/NR and PANI@CNs/NR nanocomposites. Composites reinforced with PANI and PANI@CNs nanohybrids present better tensile strength and higher Young's modulus than pure NR, indicating the reinforcement effect of these fillers. Compared with pure NR (1.7 MPa), the tensile strength of PANI@CNs/NR (6.1 MPa) is increased by 267.3%, while the tensile strength of PANI/NR (3.4 MPa) is increased by 103.0%. Meanwhile, the Young's modulus of PANI@CNs/NR is 10.7 MPa, which is 29.7 times of pure NR (0.4 MPa) and 4.6 times of PANI/NR (2.3 MPa). The results indicate that PANI@CNs nanohybrids is a much more efficient reinforcement filler for NR because of the high strength and modulus of CNs. On the other hand, improved dispersity of PANI@CNs (as shown in Figure S4 in the Supporting Information), which benefited from the biotemplate effect of CNs, might play an important role in enhancement of mechanical properties of the NR based composites. In addition, the elongation at break of PANI/NR and PANI@CNs/NR decreases compared to the pure NR, which is common for filled composites. The results demonstrate that the combination of biotemplate synthesis and latex cocoagulation method can improve the electrical conductivity as well as mechanical performance of NR-based composites simultaneously.

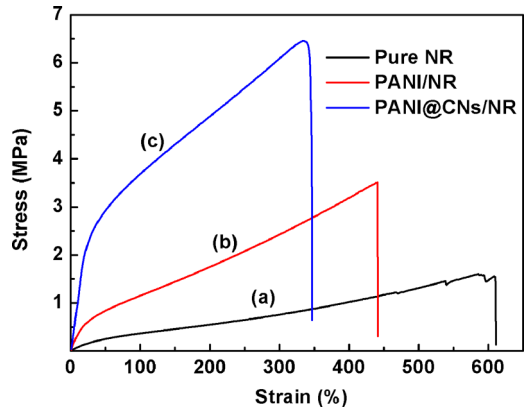

Figure 7. Representative stress−strain curves of the (a) pure NR, (b) PANI/NR (15/100 wt./wt.) and (c) PANI@CNs/NR (15/10/100 wt./wt./wt.) nanocomposites.

CONCLUSIONS

In this work, we report a facile and effective strategy to prepare PANI@CNs/NR nanocomposites with a 3D hierarchical multiscale structure by combination of the biotemplate synthesis of PANI and latex cocoagulation method. The biotemplate sythnsized PANI@CNs nanohybrids with high aspect ratio and well dispersity self-assembled onto NR latex microspheres and organized into a 3D hierarchical conductive structure in NR matrix. The fabrication of this 3D hierarchical structure significantly improved the electrical conductivity and mechanical properties of the composites simultaneously. The electrical conductivity of PANI@CNs/NR nanocomposites containing 5 phr PANI showed 11 orders of magnitude higher than that of the PANI/NR composites at the same loading fraction. This work provides a new method to enhance the conductivity and mechanical properties of the NR-based composites simultaneously by incorporation of cheap, nonconducting, renewable and biodegradable CNs, promoting the functional use of natural polymers and development of novel antistatic and electromagnetic shielding materials. We believe that this approach can be used not only for PANI and NR matrix but also for other conductive fillers and emulsion-based polymers.

ASSOCIATED CONTENT

Supporting Information

AFM image of PANI@CNs nanohybrids; high-magnification optical microscope images of NR latex, neat PANI, PANI@CNs nanohybrids, PANI/NR latex, and PANI@CNs/NR latex mixture; UV−vis spectra of the proteins extracted from NR latex; UV−vis spectra of BSA, neat PANI, and BSA-stabilized PANI; digital photographs of neat PANI and BSA-stabilized PANI; SEM images of freeze-fractured cross sections of PANI/NR and PANI@CNs/NR; table of mechanical property of pure NR, PANI/NR, and PANI@CNs/NR nanocomposites. This material is available free of charge via the Internet at http://pubs.acs.org.

AUTHOR INFORMATION

Corresponding Author

*E-mail: xxzwwh@scu.edu.cn. Tel: +86-28-85460607. Fax: +86-28-85402465.

Notes

The authors declare no competing financial interest.

ACKNOWLEDGMENTS

The authors thank the National Science Foundation of China (51203105 and 51473100) for financial support.

REFERENCES

(1) Ma, P. C.; Liu, M. Y.; Zhang, H.; Wang, S. Q.; Wang, R.; Wang, K.; Wong, Y. K.; Tang, B. Z.; Hong, S. H.; Paik, K. W.; Kim, J. K. Enhanced Electrical Conductivity of Nanocomposites Containing Hybrid Fillers of Carbon Nanotubes and Carbon Black. *ACS Appl. Mater. Interfaces* **2009**, *1*, 1090−1096.

(2) Maiti, S.; Shrivastava, N. K.; Suin, S.; Khatu, B. B. Polystyrene/MWCNT/Graphite Nanoplate Nanocomposites: Efficient Electromagnetic Interference Shielding Material through Graphite Nanoplate-MWCNT-Graphite Nanoplate Networking. *ACS Appl. Mater. Interfaces* **2013**, *5*, 4712−4724.

(3) Shin, M. K.; Oh, J.; Lima, M.; Kozlov, M. E.; Kim, S. J.; Baughman, R. H. Elastomeric Conductive Composites Based on Carbon Nanotube Forests. *Adv. Mater.* **2010**, *22*, 2663−2667.

(4) Mahendia, S.; Tomar, A.; Kumar, S. Electrical Conductivity and Dielectric Spectroscopic Studies of PVA-Ag Nanocomposite Films. *J. Alloys Compd.* **2010**, *508*, 406−411.

(5) Chen, D.; Miao, Y. E.; Liu, T. X. Electrically Conductive Polyaniline/Polyimide Nanofiber Membranes Prepared via a Combination of Electrospinning and Subsequent In situ Polymerization Growth. *ACS Appl. Mater. Interfaces* **2013**, *5*, 1206−1212.

(6) Romo-Uribe, A.; Arizmendi, L.; Romero-Guzmán, M. E.; Sepúlveda-Guzmán, S.; Cruz-Silva, R. Electrospun Nylon Nanofibers as Effective Reinforcement to Polyaniline Membranes. *ACS Appl. Mater. Interfaces* **2009**, *1*, 2502−2508.

(7) Shi, Z.; Zang, S.; Jiang, F.; Huang, L.; Lu, D.; Ma, Y.; Yang, G. In Situ Nano-assembly of Bacterial Cellulose–Polyaniline Composites. *RSC Adv.* **2012**, *2*, 1040–1046.
(8) Zhang, X.; He, Q.; Gu, H.; Colorado, H. A.; Wei, S.; Guo, Z. Flame-Retardant Electrical Conductive Nanopolymers Based on Bisphenol F Epoxy Resin Reinforced with Nano Polyanilines. *ACS Appl. Mater. Interfaces* **2013**, *5*, 898–910.
(9) Tkalya, E.; Ghislandi, M.; Thielemans, W.; Schoot, P. V.; With, G.; Koning, C. Cellulose Nanowhiskers Templating in Conductive Polymer Nanocomposites Reduces Electrical Percolation Threshold 5-Fold. *ACS Macro Lett.* **2013**, *2*, 157–163.
(10) Araujo, J. R.; Adamo, C. B.; Rocha, W. F. C.; Silva, M. V. C.; Carozo, V.; Calil, V. L.; Paoli, M. D. Elastomer Composite Based on EPDM Reinforced with Polyaniline Coated Curaua Fibers Prepared by Mechanical Mixing. *J. Appl. Polym. Sci.* **2014**, DOI: 10.1002/APP.40056.
(11) Silva, M. J.; Sanches, A. O.; Medeiros, E. S.; Mattoso, L. H. C.; McMahan, C. M.; Malmonge, J. A. Nanocomposites of Natural Rubber and Polyaniline-Modified Cellulose Nanofibrils. *J. Therm. Anal. Calorim.* **2014**, *117*, 387–392.
(12) Liao, K. H.; Qian, Y.; Macosko, C. W. Ultralow Percolation Graphene/Polyurethane Acrylate Nanocomposites. *Polymer* **2012**, *53*, 3756–3761.
(13) Zhang, M.; Jia, W.; Chen, X. Influences of Crystallization Histories on PTC/NTC Effects of PVDF/CB Composites. *J. Appl. Polym. Sci.* **1996**, *62*, 743–747.
(14) Mao, C.; Zhu, Y.; Jiang, W. Design of Electrical Conductive Composites: Tuning the Morphology to Improve the Electrical Properties of Graphene Filled Immiscible Polymer Blends. *ACS Appl. Mater. Interfaces* **2012**, *4*, 5281–5286.
(15) Qi, X. Y.; Yan, D.; Jiang, Z.; Cao, Y. K.; Yu, Z. Z.; Yavari, F.; Koratkar, N. Enhanced Electrical Conductivity in Polystyrene Nanocomposites at Ultra-Low Graphene Content. *ACS Appl. Mater. Interfaces* **2011**, *3*, 3130–3133.
(16) Etika, K. C.; Liu, L.; Hess, L. A.; Grunlan, J. C. The Influence of Synergistic Stabilization of Carbon Black and Clay on the Electrical and Mechanical Properties of Epoxy Composites. *Carbon* **2009**, *47*, 3128–3136.
(17) Liu, L.; Grunlan, J. C. Clay Assisted Dispersion of Carbon Nanotubes in Conductive Epoxy Nanocomposites. *Adv. Funct. Mater.* **2007**, *17*, 2343–2348.
(18) Zhou, Z. H.; Lu, C. .H.; Wu, X. D.; Xinxin g Zhang, X. X. Cellulose Nanocrystals as a Novel Support for CuO Nanoparticles Catalysts: Facile Synthesis and Their Application to 4-nitrophenol Reduction. *RSC Adv.* **2013**, *3*, 26066–26073.
(19) Wu, X.; Lu, C.; Zhang, W.; Yuan, G.; Xiong, R.; Zhang, X. A Novel Reagentless Approach For Synthesizing Cellulose Nanocrystal-Supported Palladium Nanoparticles with Enhanced Catalytic Performance. *J. Mater. Chem. A* **2013**, *1*, 8645–8652.
(20) Wu, X.; Lu, C.; Zhou, Z.; Yuan, G.; Xiong, R.; Zhang, X. Green Synthesis and Formation Mechanism of Cellulose Nanocrystal-Supported Gold Nanoparticles with Enhanced Catalytic Performance. *Environmental Science: Nano* **2014**, *1*, 71–79.
(21) Shi, X.; Zhang, L.; Cai, J.; Cheng, G.; Zhang, H.; Li, J.; Wang, X. A Facile Construction of Supramolecular Complex from Polyaniline and Cellulose in Aqueous System. *Macromolecules* **2011**, *44*, 4565–4568.
(22) Zhou, Z. H.; Zhang, X. X.; Lu, C. H.; Lan, L. D.; Yuan, G. P. Polyaniline-Decorated Cellulose Aerogel Nanocomposite with Strong Interfacial Adhesion and Enhanced Photocatalytic Activity. *RSC Adv.* **2014**, *4*, 8966–8972.
(23) Gu, B. K.; Ismail, Y. A.; Spinks, G. M.; Kim, S. I.; So, I.; Kim, S. J. A Linear Actuation of Polymeric Nanofibrous Bundle for Artificial Muscles. *Chem. Mater.* **2009**, *21*, 511–515.
(24) Miao, Y. E.; Fan, W.; Chen, D.; Liu, T. X. High-Performance Supercapacitors Based on Hollow Polyaniline Nanofibers by Electrospinning. *ACS Appl. Mater. Interfaces* **2013**, *5*, 4423–4428.
(25) Xia, Y.; Zhu, H. Polyaniline Nanofiber-Reinforced Conducting Hydrogel with Unique pH-Sensitivity. *Soft Matter.* **2011**, *7*, 9388–9393.
(26) Lin, Z.; Guan, Z.; Huang, Z. New Bacterial Cellulose/Polyaniline Nanocomposite Film with One Conductive Side through Constrained Interfacial Polymerization. *Ind. Eng. Chem. Res.* **2013**, *52*, 2869–2874.
(27) Liu, D. Y.; Sui, G. X.; Bhattacharyya, D. Synthesis and Characterisation of Nanocellulose-Based Polyaniline Conducting Films. *Compos. Sci. Technol.* **2014**, *99*, 31–36.
(28) Yan, D.; Zhang, H. B.; Jia, Y.; Hu, J.; Qi, X. Y.; Zhang, Z.; Yu, Z. Z. Improved Electrical Conductivity of Polyamide 12/Graphene Nanocomposites with Maleated Polyethylene-Octene Rubber Prepared by Melt Compounding. *ACS Appl. Mater. Interfaces* **2012**, *4*, 4740–4745.
(29) Wu, C.; Huang, X.; Wang, G.; Lv, L.; Chen, G.; Li, G.; Jiang, P. Highly Conductive Nanocomposites with Three-Dimensional, Compactly Interconnected Graphene Networks via a Self-Assembly Process. *Adv. Funct. Mater.* **2013**, *23*, 506–513.
(30) Yang, L.; Wang, Z.; Ji, Y.; Wang, J.; Xue, G. Highly Ordered 3D Graphene-Based Polymer Composite Materials Fabricated by "Particle-Constructing" Method and Their Outstanding Conductivity. *Macromolecules* **2014**, *47*, 1749–1756.
(31) Zhan, Y.; Lavorgna, M.; Buonocore, G.; Xia, H. Enhancing Electrical Conductivity of Rubber Composites by Constructing Interconnected Network of Self-assembled Graphene with Latex Mixing. *J. Mater. Chem.* **2012**, *22*, 10464–10468.
(32) Potts, J. R.; Shankar, O.; Du, L.; Ruoff, R. S. Processing-Morphology-Property Relationships and Composite Theory Analysis of Reduced Graphene Oxide/Natural Rubber Nanocomposites. *Macromolecules* **2012**, *45*, 6045–6055.
(33) Pham, V. H.; Dang, T. T.; Hur, S. H.; Kim, E. J.; Chung, J. S. Highly Conductive Poly(methyl methacrylate) (PMMA)-Reduced Graphene Oxide Composite Prepared by Self-Assembly of PMMA Latex and Graphene Oxide through Electrostatic Interaction. *ACS Appl. Mater. Interfaces* **2012**, *4*, 2630–2636.
(34) Wang, H.; Zhu, E.; Yang, J.; Zhou, P.; Sun, D.; Tang, W. Bacterial Cellulose Nanofiber-Supported Polyaniline Nanocomposites with Flake-Shaped Morphology as Supercapacitor Electrodes. *J. Phys. Chem. C* **2012**, *116*, 13013–13019.
(35) Hu, W.; Chen, S.; Yang, Z.; Liu, L.; Wang, H. Flexible Electrically Conductive Nanocomposite Membrane Based on Bacterial Cellulose and Polyaniline. *J. Phys. Chem. B* **2011**, *115*, 8453–8457.
(36) Gu, Y.; Huang, J. Nanographite Sheets Derived From Polyaniline Nanocoating of Cellulose Nanofibers. *Mater. Chem. Phys.* **2013**, *48*, 429–434.
(37) Hu, W.; Liu, S.; Chen, S.; Wang, H. Preparation and Properties of Photochromic Bacterial Cellulose Nanofibrous Membranes. *Cellulose* **2011**, *18*, 655–661.
(38) Crean (neé Lynam), C.; Lahiff, E.; Gilmartin, N.; Diamond, D.; O'Kennedy, R. Polyaniline Nanofibres as Templates for the Covalent Immobilisation of Biomolecules. *Synth. Met.* **2011**, *161*, 285–292.
(39) Lu, Y.; Song, Y.; Wang, F. Thermoelectric Properties of Graphene Nanosheets-Modified Polyaniline Hybrid Nanocomposites by an In Situ Chemical Polymerization. *Mater. Chem. Phys.* **2013**, *138*, 238–244.